Experimental Realization of a Controlled-NOT Gate with Four-Photon Six-Qubit Cluster States

Wei-Bo Gao,[1] Ping Xu,[1] Xing-Can Yao,[1] Otfried Gühne,[2,3] Adán Cabello,[4] Chao-Yang Lu,[1] Cheng-Zhi Peng,[1] Zeng-Bing Chen,[1] and Jian-Wei Pan[1,5]

[1] *Hefei National Laboratory for Physical Sciences at Microscale and Department of Modern Physics, University of Science and Technology of China, Hefei, Anhui 230026, China*
[2] *Institut für Quantenoptik und Quanteninformation, Österreichische Akademie der Wissenschaften, Technikerstraße 21A, A-6020 Innsbruck, Austria*
[3] *Institut für theoretische Physik, Universität Innsbruck, Technikerstraße 25, A-6020 Innsbruck, Austria*
[4] *Departamento de Física Aplicada II, Universidad de Sevilla, E-41012 Sevilla, Spain*
[5] *Physikalisches Institut, Ruprecht-Karls-Universität Heidelberg, Philosophenweg 12, 69120 Heidelberg, Germany*

(Received 19 June 2009; published 13 January 2010)

We experimentally demonstrate an optical controlled-NOT (CNOT) gate with arbitrary single inputs based on a 4-photon 6-qubit cluster state entangled both in polarization and spatial modes. We first generate the 6-qubit state, and then, by performing single-qubit measurements, the CNOT gate is applied to arbitrary single input qubits. To characterize the performance of the gate, we estimate its quantum process fidelity and prove its entangling capability. In addition, our results show that the gate cannot be reproduced by local operations and classical communication. Our experiment shows that such hyper-entangled cluster states are promising candidates for efficient optical quantum computation.

DOI: 10.1103/PhysRevLett.104.020501 PACS numbers: 03.67.Lx, 03.67.Bg, 42.50.Dv, 42.50.Ex

Introduction.—Cluster states not only provide a useful model to study multiparticle entanglement [1,2], but also have applications in quantum communication [3], quantum nonlocality [4–6], and quantum error correction [7]. Specifically, they play a crucial role in one-way quantum computation [8], which is a promising approach towards scalable quantum computation. Considerable efforts have been made toward generating and characterizing multiparticle cluster states, especially in linear optics [9–11]. Recently, some 4-photon cluster states and one-way quantum computation based on them have been experimentally demonstrated [12–14]. Also, the 6-photon cluster state has been reported [15]. An efficient way to extend the number of qubits without increasing the number of particles is entangling in various degrees of freedom [16–23]. This type of entanglement is called hyper-entanglement [17,24], which can have a high generation rate and fidelity, and thus are particularly suitable for one-way quantum computation [20,25].

In this Letter, we report on the creation of a 4-photon 6-qubit cluster state entangled in photons' polarization and spatial modes and an optical controlled-NOT (CNOT) gate with arbitrary single-qubit inputs based on the state. To characterize our gate, we obtain an estimation of the quantum process fidelity and entangling capability [26,27]. Moreover, the experimental results show that the performance of the gate cannot be reproduced by local operations and classical communication [27].

Cluster states are defined as eigenstates of certain sets of local observables. For instance, an N-qubit linear cluster state is the eigenstate (with eigenvalue $+1$) of the N observables $X_1Z_2, Z_1X_2Z_3, \ldots, Z_{N-1}X_N$, where X_i and Z_j are Pauli matrices on the qubits i and j, respectively. Given a cluster state, one-way quantum computation can be performed by making consecutive single-qubit measurements in the basis $B_k(\alpha) = \{|\alpha_+\rangle_k, |\alpha_-\rangle_k\}$, where $|\alpha_\pm\rangle_k = (|0\rangle_k \pm e^{i\alpha}|1\rangle_k)/\sqrt{2}$ ($\alpha \in \mathbb{R}$), followed by feed-forward operations depending on the measurement results. This measurement basis determines a rotation $R_z(\alpha) = \exp(i\alpha Z/2)$, followed by a Hadamard operation $H = (X + Z)/\sqrt{2}$ on the encoded qubits. As depicted in Fig. 1, based on a linear-type 6-qubit cluster state $|\mathrm{LC}_6\rangle$, measurements on qubits 5, 1, 6, 4 in the basis $\{B_5(\alpha), B_1(\beta), B_6(\alpha'), B_4(\beta')\}$ will give an output state on qubits 2, 3 with $(\mathbb{1} \otimes H)\mathrm{CNOT}[R_x(\beta')R_z(\alpha') \otimes HR_x(\beta)R_z(\alpha)]|\tilde{0}\rangle_2|\tilde{0}\rangle_3$,

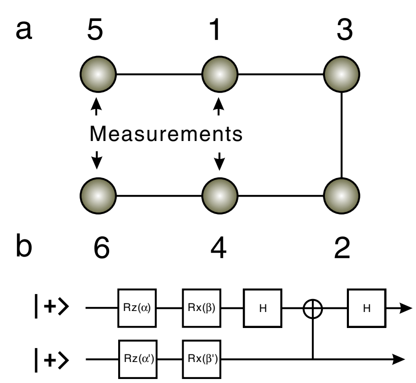

FIG. 1 (color online). A one-way quantum CNOT gate based on cluster states. (a) 4-photon 6-qubit linear cluster state. Qubits 1, 2, 3, 4 are polarization qubits, and qubits 5, 6 are spatial qubits. By implementing single-photon measurements and feed-forward operations depending on the measurement results, the input qubits are transmitted through a deterministic CNOT gate. (b) Corresponding quantum circuit. $R_z(\alpha) = \exp(i\alpha Z/2)$, $R_x(\beta) = \exp(i\beta X/2)$, and H denotes a Hadamard gate.

where $|\tilde{0}\rangle = \frac{1}{\sqrt{2}}(|0\rangle + |1\rangle)$. $R_x(\beta')R_z(\alpha')$ and $HR_x(\beta)R_z(\alpha)$ are sufficient to realize arbitrary single-qubit rotations; thus, after compensating the H gate behind the CNOT gate, a CNOT gate with arbitrary single-qubit inputs can be achieved. Qubits 2 and 3 are, respectively, the control and target qubits.

Preparation.—The schematic setup for preparing the 4-photon 6-qubit cluster state is depicted in Fig. 2. We use spontaneous down conversion to produce the desired 4 photons. With the help of polarizing beam splitters (PBSs), half-wave plates (HWPs), and conventional photon detectors, we prepare a 4-qubit cluster state

$$|C_4\rangle = \frac{1}{2}[|+\rangle_1|H\rangle_3(|H\rangle_2|+\rangle_4 + |V\rangle_2|-\rangle_4) + |-\rangle_1|V\rangle_3(|H\rangle_2|+\rangle_4 - |V\rangle_2|-\rangle_4)], \quad (1)$$

where $|H\rangle$ ($|V\rangle$) represents the state with the horizontal (vertical) polarization and $|\pm\rangle = 1/\sqrt{2}(|H\rangle \pm |V\rangle)$. The scheme for preparing $|C_4\rangle$ is similar to the one introduced in [14]. After creating $|C_4\rangle$, we place two PBSs in the outputs of photons 1 and 4, as depicted in Fig. 2(a). Since a PBS transmits H and reflects V polarization, H-polarized photons will follow one path and V-polarized photons will follow the other. In this way, the spatial qubits are added onto the polarization qubits: $\alpha|H\rangle_1 + \beta|V\rangle_1 \rightarrow \alpha|HH'\rangle_1 + \beta|VV'\rangle_1$, with the levels denoted as $|H'\rangle$ for the first path and $|V'\rangle$ for the latter path [see Fig. 2(a)]. This process is equivalent to a controlled-phase gate between the polarization qubit and a spatial qubit $\frac{1}{\sqrt{2}}(|H'\rangle + |V'\rangle)$ up to single-qubit unitary transformation.

If we consider $|H'\rangle_{1,4}$ as $|0\rangle_{5,6}$, $|V'\rangle_{1,4}$ as $|1\rangle_{5,6}$ and $|H\rangle \leftrightarrow |0\rangle$, $|V\rangle \leftrightarrow |1\rangle$, the state will be expressed as

$$|\widetilde{\mathrm{LC}}_6\rangle = \frac{1}{2\sqrt{2}}[(|0\rangle_5|0\rangle_1 + |1\rangle_5|1\rangle_1)|0\rangle_3(|\tilde{0}\rangle_2|0\rangle_4|0\rangle_6 + |\tilde{1}\rangle_2|1\rangle_4|1\rangle_6) + (|0\rangle_5|0\rangle_1 - |1\rangle_5|1\rangle_1)|1\rangle_3 \times (|\tilde{1}\rangle_2|0\rangle_4|0\rangle_6 + |\tilde{0}\rangle_2|1\rangle_4|1\rangle_6)], \quad (2)$$

where $|\tilde{0}\rangle = \frac{1}{\sqrt{2}}(|0\rangle + |1\rangle)$, $|\tilde{1}\rangle = \frac{1}{\sqrt{2}}(|0\rangle - |1\rangle)$. State (2) is equivalent to a 6-qubit linear cluster state up to two single-qubit Hadamard transformations, H_5 and H_6.

To implement the required measurements of one-way quantum computation and estimate the fidelity of the state, we need to project the spatial qubits onto $|\alpha_\pm\rangle_k = (|0\rangle_k \pm e^{i\alpha}|1\rangle_k)/\sqrt{2}$. The required devices are shown in Fig. 2(b). When $\alpha \neq 0$, the measurements are performed by matching different spatial modes on a common BS, and the phase is determined by the difference between the optical path length of two input modes. Here single-photon interferometers are required in the experiment. To achieve a high stability for the single-photon interferometer, we have constructed an ultrastable Sagnac setup [28,29] [see Fig. 2(c)], which can be stable for almost 10 hours [22]. We have first designed a special crystal combining a PBS

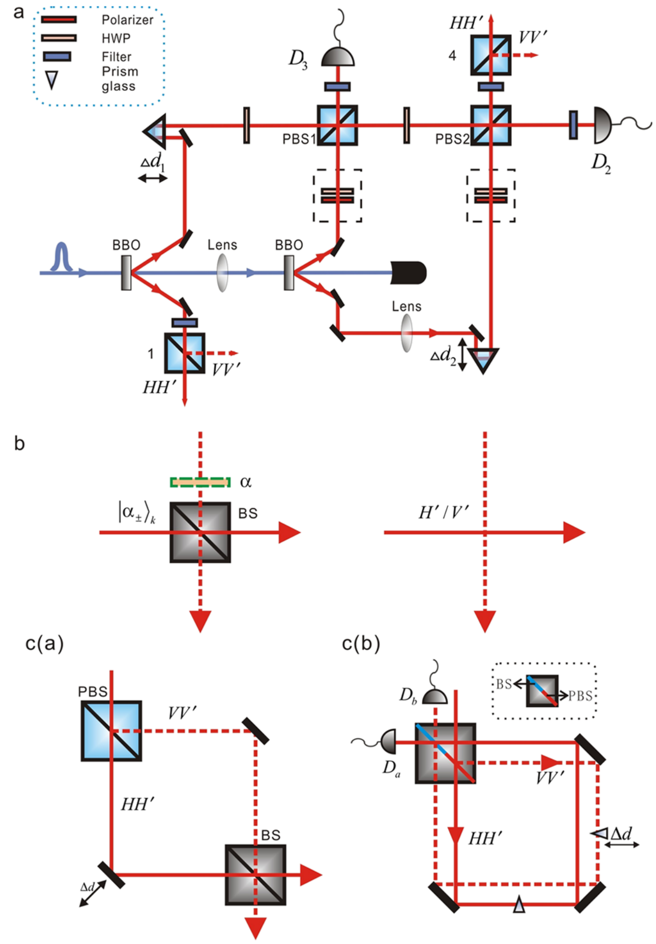

FIG. 2 (color online). Schematic of the experimental setup. (a) The setup to generate the required entanglement state. Femtosecond laser pulses (≈200 fs, 76 MHz, 788 nm) are converted to ultraviolet pulses through a frequency doubler LiB_3O_5 (LBO) crystal (not shown). The pulses go through two main β-barium borate (BBO) crystals (2 mm), generating two pairs of photons. The observed twofold coincident count rate is about 2.6×10^4/s. Two polarizers are placed in the arms of the second entanglement pair in order to prepare the required single-photon source. (b) Setups for projecting the spatial qubits onto $|\alpha_\pm\rangle_k = (|0\rangle_k \pm e^{i\alpha}|1\rangle_k)/\sqrt{2}$, H' and V'. (c) Ultrastable Sagnac single-photon interferometer. Details are discussed in the text.

and a beam splitter (BS). When an input photon enters the interferometer, it is split by the PBS. The H component of the photon is transmitted and propagates counterclockwise through the interferometer; the V component is reflected and propagates clockwise. The two spatial modes match at the BS and the interference occurs there. After being detected by two detectors D_a and D_b, the output states are, respectively, projected onto $\frac{1}{\sqrt{2}}(|0\rangle + e^{i\alpha}|1\rangle)$ and $\frac{1}{\sqrt{2}}(|0\rangle - e^{i\alpha}|1\rangle)$.

Fidelity.—To characterize the quality of the generated state, we estimate its fidelity $F = \langle\widetilde{\mathrm{LC}}_6|\rho_{\mathrm{exp}}|\widetilde{\mathrm{LC}}_6\rangle$. F is equal to 1 for an ideal state and 1/64 for a completely mixed state. We consider an observable B with the property that $\mathrm{tr}(B\rho_{\mathrm{exp}}) \leq \mathrm{tr}(|\widetilde{\mathrm{LC}}_6\rangle\langle\widetilde{\mathrm{LC}}_6|\rho_{\mathrm{exp}}) = F$, which implies that the lower bound of the fidelity can be obtained by measuring observable B. Using the method introduced in [30], we construct the observable B as

$$B = \frac{1}{32}\{4(P_{51}^- X_3 Z_2 P_{46}^+ + P_{51}^- Y_3 Y_2 P_{46}^-) + 2[P_{51}^-(X_3 \mathbb{1}_2 X_4 X_6 - Y_3 X_2 Y_4 X_6 - X_3 \mathbb{1}_2 Y_4 Y_6 - Y_3 X_2 X_4 Y_6)] + (X_5 Y_1 + Y_5 X_1)[2(Y_3 Z_2 P_{46}^+ - X_3 Y_2 P_{46}^-) + (Y_3 \mathbb{1}_2 X_4 X_6 - Y_3 \mathbb{1}_2 Y_4 Y_6 + X_3 X_2 X_4 Y_6 + X_3 X_2 Y_4 X_6)]\}, \quad (3)$$

where $P_{i,j}^{\pm} = |00\rangle_{ij}\langle 00| \pm |11\rangle_{ij}\langle 11|$. Experimental values of the required measurement settings are given in Table I, from which we obtain

$$F \geq \mathrm{tr}(B\rho_{\mathrm{exp}}) = 0.61 \pm 0.01, \quad (4)$$

which is clearly higher than 0.5, and thus proves the existence of genuine 6-qubit entanglement in our state [31].

Entangling capability.—To evaluate the performance of the CNOT gate, we obtain the upper and lower bound of the quantum process fidelity F_{process}. As discussed in [26], F_{process} can be estimated as

$$F_{zz} + F_{xx} - 1 \leq F_{\mathrm{process}} \leq \min(F_{zz}, F_{xx}), \quad (5)$$

where the fidelities are defined as

$$F_{zz} = 1/4[P(HH|HH) + P(HV|HV) + P(VV|VH) + P(VH|VV)],$$
$$F_{xx} = 1/4[P(++|++) + P(--|+-) + P(-+|-+) + P(+-|--)], \quad (6)$$

where each P represents the probability of obtaining the corresponding output state under the specified input state. Experimentally, when $\{\alpha', \beta', \alpha, \beta\}$ take the values $\{\pm\pi/2, \pm\pi/2, (0,\pi), (0,\pi)\}$, both the control and target input qubit will lie on the basis $|H\rangle/|V\rangle$, and when $\{\alpha', \beta', \alpha, \beta\}$ take the values $\{(0,\pi), (0,\pi), \pm\pi/2, \pm\pi/2\}$, they will lie on the basis $|+\rangle/|-\rangle$. The results are depicted in Fig. 3. F_{zz} (F_{xx}) is 79% ± 2% (78% ± 2%); thus, the fidelity of the gate lies between 57% ± 3% and 78% ± 2%.

Since the fidelity of entanglement generation is at least equal to the process fidelity, the lower bound of the process fidelity defines a lower bound of the entanglement capability of the gate [26]. In terms of the concurrence C which the gate can generate from product state inputs, the minimal entanglement capability of the gate is given by

$$C \geq 2F_{\mathrm{process}} - 1 \geq 2(F_{zz} + F_{xx}) - 3. \quad (7)$$

In our experiment, the obtained lower bound of C is 0.14 ± 0.05, confirming the entanglement capability of our gate.

Quantum parallelism.—It was shown that a quantum CNOT gate is capable of simultaneously performing the logical functions of three distinct conditional local opera-

TABLE I. Experimental values of the observables for the fidelity estimation of $|\widetilde{LC}_6\rangle$. Each experimental value is obtained by measuring in 400 seconds and propagated Poissonian statistics of raw detection events are considered.

Observable	Value	Observable	Value
$X_5Y_1Y_3\mathbb{1}_2X_4X_6$	0.58 ± 0.04	$X_5Y_1Y_3\mathbb{1}_2Y_4Y_6$	−0.63 ± 0.04
$X_5Y_1X_3X_2Y_4X_6$	0.58 ± 0.04	$X_5Y_1X_3X_2X_4Y_6$	0.60 ± 0.04
$Y_5X_1Y_3\mathbb{1}_2X_4X_6$	0.55 ± 0.04	$Y_5X_1Y_3\mathbb{1}_2Y_4Y_6$	−0.56 ± 0.04
$Y_5X_1X_3X_2Y_4X_6$	0.57 ± 0.04	$Y_5X_1X_3X_2X_4Y_6$	0.60 ± 0.04
$P_{5,1}^-X_3Z_2P_{4,6}^+$	0.64 ± 0.04	$P_{5,1}^-Y_3Y_2P_{4,6}^-$	0.65 ± 0.04
$P_{5,1}^-X_3\mathbb{1}_2X_4X_6$	0.58 ± 0.03	$P_{5,1}^-Y_3X_2Y_4X_6$	−0.66 ± 0.04
$P_{5,1}^-X_3\mathbb{1}_2Y_4Y_6$	−0.57 ± 0.04	$P_{5,1}^-Y_3X_2X_4Y_6$	−0.58 ± 0.05
$X_5Y_1Y_3Z_2P_{4,6}^+$	0.57 ± 0.05	$X_5Y_1X_3Y_2P_{4,6}^-$	−0.65 ± 0.04
$Y_5X_1Y_3Z_2P_{4,6}^+$	0.67 ± 0.03	$Y_5X_1X_3Y_2P_{4,6}^-$	−0.58 ± 0.05

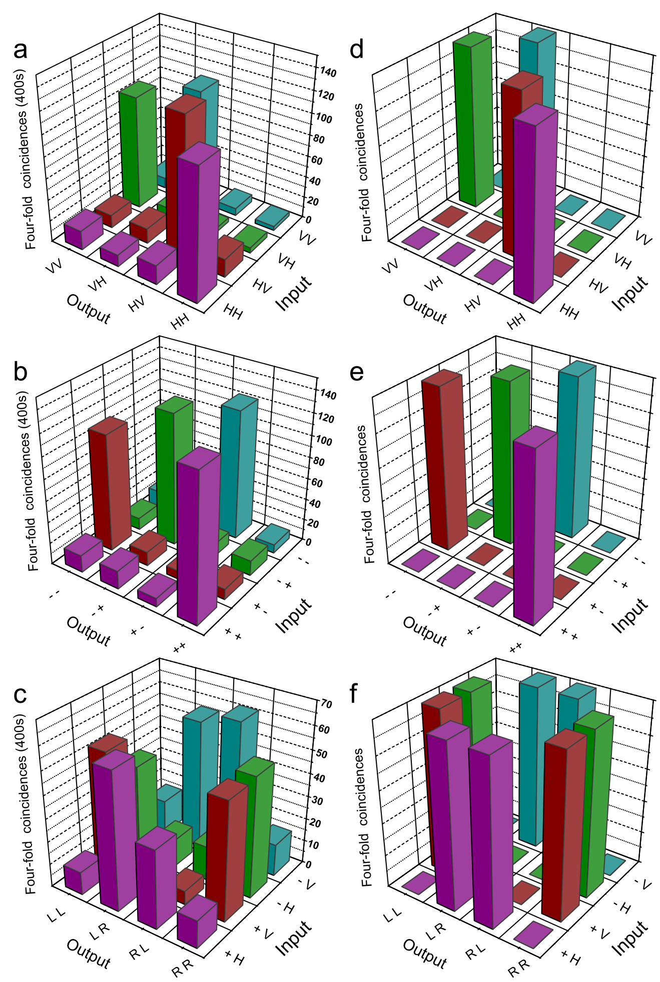

FIG. 3 (color online). Experimental evaluation of the process fidelity of the CNOT gate. In the experiment, each data is measured in 400 s. (a) The experimental data of F_{zz}, defined in the basis ($|H\rangle/|V\rangle$). (b) The experimental values of F_{xx}, defined in the basis ($|+\rangle/|-\rangle$). (c) The experimental values of F_{xz}. The input control qubit is in the basis ($|+\rangle/|-\rangle$), and the input target qubit is in the basis ($|H\rangle/|V\rangle$), while the output qubits are measured in the basis ($|R\rangle/|L\rangle$). (d) The theoretical data of F_{zz}. (e) The theoretical data of F_{xx}. (f) The theoretical data of F_{xz}.

tions, each of which can be verified by measuring a corresponding truth table of four local inputs and four local outputs [27]. If the experimental gate can effectively perform more than one local operation in parallel, one can say that quantum parallelism has been achieved, which also means that the gate cannot be reproduced by local operations and classical communication [27]. Specially, quantum parallelism will be achieved if the average fidelity of these three distinct conditional local operations exceeds 2/3, where F_{zz}, F_{xx} are two of them, and the third one is

$$F_{xz} = 1/4[P(RL/+H) + P(LR/+H) + P(RR/+V) + P(LL/+V) + P(RR/-H) + P(LL/-H) + P(RL/-V) + P(LR/-V)], \tag{8}$$

where $|R\rangle = 1/\sqrt{2}(|H\rangle + i|V\rangle)$, $|L\rangle = 1/\sqrt{2}(|H\rangle - i|V\rangle)$. F_{xz} is calculated to be 80% ± 2% [see Fig. 3(c)], so the average fidelity of the three results is 79% ± 1%, obviously exceeding the boundary 2/3 and thus proving quantum parallelism in our gate.

The imperfection of the fidelity is mainly caused by the noise in the state generation and the imperfect interferometers. Moreover, in Hofmann's theoretical scheme of process estimation, the input states of the tested gate should be perfect [26,27], while our initial input qubits are nonideal due to the imperfection of the experimental cluster state, which will affect the accuracy of the process estimation to some extent.

Conclusion and discussion.—In our experiment, we have generated a four-photon six-qubit cluster state entangled in the photons' polarization and spatial modes. In order to create new types of cluster states and perform new one-way quantum computations, our method can be extended to more photons by increasing the power of pump light [15] or to more degrees of freedom [17]. With the latter approach, the complexity of the measurement apparatus may increase.

Based on the six-qubit state, we have given a proof-of-principle demonstration of one-way quantum CNOT gate with arbitrary single-qubit inputs. Our results show that photons' polarization and spatial degrees of freedom are both promising resources for efficient optical quantum computation. As a general procedure for application, we can first generate a cluster state entangled in photons' polarization modes. Then, extra spatial qubits can be planted onto the polarization qubits. The additional spatial qubits can be used to perform local rotations, as shown in our experiment. More recently, it has been shown that by making use of additional degrees of freedom, generalized quantum measurements (POVMs) instead of projective measurements can largely extend the quantum computational power of cluster states [32]. It remains an open question how to most efficiently exploit different degrees of freedom of photons for quantum computation.

Finally, we did not use active feed-forward operation in the present experiment, and this reduced the success rate of the computation by a factor of 2 for each measurement of qubits compared to deterministic gate operations. However, this suffices for a proof-of-principle demonstration. Feed-forward operations have been developed in Refs. [25,33]. By making use of delay fibers and Pockels cells driven by the output signals of detectors, one can perform the feed-forward operations, which can be readily combined with our experiment in the future.

This work is supported by the NNSF of China, the CAS, the National Fundamental Research Program (under Grant No. 2006CB921900), the European Commission through the ERC grant and the STREP project HIP, the FWF (START grant), the EU (OLAQUI, QICS, SCALA), the MCI Project No. FIS2008-05596, and the Junta de Andalucía Excellence Project No. P06-FQM-02243.

[1] H. J. Briegel and R. Raussendorf, Phys. Rev. Lett. **86**, 910 (2001).
[2] M. Hein, J. Eisert, and H. J. Briegel, Phys. Rev. A **69**, 062311 (2004).
[3] R. Cleve, D. Gottesman, and H.-K. Lo, Phys. Rev. Lett. **83**, 648 (1999).
[4] O. Gühne *et al.*, Phys. Rev. Lett. **95**, 120405 (2005).
[5] V. Scarani *et al.*, Phys. Rev. A **71**, 042325 (2005).
[6] A. Cabello, Phys. Rev. Lett. **95**, 210401 (2005).
[7] D. Schlingemann and R. F. Werner, Phys. Rev. A **65**, 012308 (2001).
[8] R. Raussendorf and H. J. Briegel, Phys. Rev. Lett. **86**, 5188 (2001).
[9] M. A. Nielsen, Phys. Rev. Lett. **93**, 040503 (2004).
[10] D. E. Browne and T. Rudolph, Phys. Rev. Lett. **95**, 010501 (2005).
[11] T. P. Bodiya and L.-M. Duan, Phys. Rev. Lett. **97**, 143601 (2006).
[12] P. Walther *et al.*, Nature (London) **434**, 169 (2005); Phys. Rev. Lett. **95**, 020403 (2005).
[13] N. Kiesel *et al.*, Phys. Rev. Lett. **95**, 210502 (2005).
[14] Y. Tokunaga *et al.*, Phys. Rev. Lett. **100**, 210501 (2008).
[15] C.-Y. Lu *et al.*, Nature Phys. **3**, 91 (2007).
[16] A. Mair *et al.*, Nature (London) **412**, 313 (2001).
[17] J. T. Barreiro *et al.*, Phys. Rev. Lett. **95**, 260501 (2005).
[18] C. Schuck *et al.*, Phys. Rev. Lett. **96**, 190501 (2006).
[19] G. Vallone *et al.*, Phys. Rev. Lett. **98**, 180502 (2007).
[20] K. Chen *et al.*, Phys. Rev. Lett. **99**, 120503 (2007).
[21] H. S. Park *et al.*, Opt. Express **15**, 17960 (2007).
[22] W.-B. Gao *et al.*, arXiv:quant-ph/08094277.
[23] B. P. Lanyon *et al.*, Nature Phys. **5**, 134 (2009).
[24] P. G. Kwiat, J. Mod. Opt. **44**, 2173 (1997).
[25] G. Vallone *et al.*, Phys. Rev. Lett. **100**, 160502 (2008).
[26] H. F. Hofmann, Phys. Rev. Lett. **94**, 160504 (2005).
[27] H. F. Hofmann, Phys. Rev. A **72**, 022329 (2005).
[28] T. Nagata *et al.*, Science **316**, 726 (2007).
[29] M. P. Almeida *et al.*, Science **316**, 579 (2007).
[30] O. Gühne *et al.*, Phys. Rev. A **76**, 030305(R) (2007).
[31] G. Tóth and O. Gühne, Phys. Rev. Lett. **94**, 060501 (2005).
[32] D. N. Biggerstaff *et al.*, Phys. Rev. Lett. **103**, 240504 (2009).
[33] R. Prevedel *et al.*, Nature (London) **445**, 65 (2007).